http://eprints.gla.ac.uk/182741/

Deposited on: 25 March 2019

1 **De-etiolation Enhances Phototropism by Modulating NPH3 Phosphorylation**

2 **Status in *Arabidopsis***

3

4 Stuart Sullivan[1], Eros Kharshiing[2], Janet Laird[1], Tatsuya Sakai[3] and John M. Christie[1]

5

6 [1]Institute of Molecular, Cell and Systems Biology, College of Medical, Veterinary and Life Sciences,

7 Bower Building, University of Glasgow, Glasgow G12 8QQ, UK

8 [2]Department of Botany, St. Edmund's College, Shillong 793003, Meghalaya, India

9 [3]Institute of Science and Technology, Niigata University, 8050 Ninocho, Ikarashi, Nishiku, Niigata

10 950-2181, Japan

11

12 Corresponding Author: John M. Christie; Tel: +44 141 330 239; Email john.christie@glasgow.ac.uk

13

14 Running title: De-etiolation Enhances the Phototropic Growth

15

16 Keywords: *Arabidopsis thaliana*, localisation, NPH3, phosphorylation, phototropin, phototropism

17

18 Word count: Summary (231); One Sentence Summary (32); Introduction (941); Results (1,982);

19 Discussion (1,312); Materials and Methods (1,156); Acknowledgments (74); References (1,839);

20 Figure Legends (1,177); Total (8,744).

21

22

23

24   **Summary**

25   Phototropin (phot) receptor kinases play important roles in promoting plant growth by controlling

26   light-capturing processes, such as phototropism. Phototropism is mediated through the action of

27   NON-PHOTOTROPIC HYPOCOTYL 3 (NPH3), which is dephosphorylated following phot activation.

28   However, the functional significance of this early signalling event remains unclear. Here, we show

29   that the onset of phototropism in dark-grown (etiolated) seedlings of *Arabidopsis* (and in tomato)

30   is enhanced by greening (de-etiolation). Red and blue light were equally effective in promoting

31   phototropism in *Arabidopsis*, consistent with our observations that de-etiolation by phytochrome

32   or cryptochrome was sufficient to elicit phototropic enhancement. Increased responsiveness did

33   not result from an enhanced sensitivity to the phytohormone auxin nor does it involve the phot-

34   interacting protein, ROOT PHOTOTROPISM 2. Instead, de-etiolated seedlings showed attenuated

35   levels of NPH3 dephosphorylation and diminished re-localisation of NPH3 from the plasma

36   membrane during phototropism. Likewise, etiolated seedlings that lack the PHYTOCHROME-

37   INTERACTING   FACTORS   (PIFs)   PIF1,   PIF3,   PIF4   and   PIF5   displayed   reduced   NPH3

38   dephosphorylation   and   enhanced   phototropism   consistent   with   their   constitutive

39   photomorphogenic phenotype in darkness. Phototropic enhancement could also be achieved in

40   etiolated seedlings by lowering the light intensity to diminish NPH3 dephosphorylation. Thus,

41   phototropism is enhanced following de-etiolation through the modulation of a phosphorylation

42   rheostat, which in turn sustains the activity of NPH3. We propose that this dynamic mode of

43   regulation enables young seedlings to maximise their establishment under changing light

44   conditions, depending on their photoautotrophic capacity.

45

46 **Significance Statement**

47 Phototropism in flowering plants is enhanced by seedling de-etiolation and is achieved by

48 modulating a molecular rheostat that fine tunes the phosphorylation and localisation status of

49 the central phototropic signalling component, NPH3.

50

Introduction

Plants orientate the growth of their stems towards light, a response known as phototropism. Phototropism is induced by UV/blue light and is controlled by two phototropin (phot) receptor kinases, phot1 and phot2 (Fankhauser and Christie, 2015). Phot1 is the primary phototropic receptor and functions over a wide range of fluence rates, whereas phot2 activity predominates at higher light intensities (Sakai et al., 2001). It is widely accepted that phototropism results from differential cell growth across the stem brought about by an asymmetric accumulation of the phytohormone, auxin (Christie and Murphy, 2013; Liscum et al., 2014). How this lateral auxin gradient forms in response to phot activation is still not understood (Fankhauser and Christie, 2015). However, members of the NPH3/RPT2-like (NRL) family are known to play important roles (Christie et al., 2018).

Arabidopsis mutants deficient in the founding NRL member, NON-PHOTOTROPIC HYPOCOTYL 3 (NPH3), fail to show phototropism under a variety of different light conditions (Sakai and Haga, 2012; Liscum et al., 2014; Fankhauser and Christie, 2015). NPH3 appears to be instrumental in establishing the lateral auxin gradients required for phototropic growth (Haga et al., 2005; Haga et al., 2015). Its primary amino acid structure can be separated into three regions based on sequence conservation with other NRL proteins: a BTB (bric-a-brac, tramtrack and broad complex) domain at the N-terminus, an NPH3 domain, and a C-terminal coiled-coil domain (Liscum et al., 2014; Christie et al., 2018). NPH3 is reported to form part of the CUL3 RING E3 UBIQUITIN LIGASE (CRL3) complex that ubiquitinates phot1 (Roberts et al., 2011; Deng et al., 2014). Poly-ubiquitination of phot1 is associated with its degradation in response to prolonged

72   irradiation, whereas its mono-ubiquitination is proposed to initiate the internalisation of phot1

73   from the plasma membrane at low light intensities (Roberts et al., 2011).

74   NPH3, like the phots, is associated with the plasma membrane in *Arabidopsis* (Haga et al.,

75   2015). The C-terminal region, including the coiled-coil domain, appears to help localise NPH3 to

76   the plasma membrane (Inoue et al., 2008), where it interacts with phot1 (Haga et al., 2015). This

77   interaction is transiently disrupted upon irradiation and is correlated with the phosphorylation

78   status of NPH3 (Haga et al., 2015). NPH3 is phosphorylated in darkness but becomes rapidly

79   dephosphorylated when phot1 is activated by light (Pedmale and Liscum, 2007). The phosphatase

80   responsible for NPH3 dephosphorylation remains unknown but this process appears to be

81   tissue/cell autonomous (Sullivan et al., 2016). Light not only alters the phosphorylation status of

82   NPH3 but also leads to dynamic changes in its subcellular localisation. NPH3 is rapidly internalised

83   into aggregates upon phot1 activation (Haga et al., 2015). The formation of these aggregates is

84   reversible in darkness (Haga et al., 2015), as is the re-phosphorylation of NPH3 (Pedmale and

85   Liscum, 2007). However, the functional significance of these changes to NHP3's phosphorylation

86   status and localisation is not fully understood.

87   ROOT PHOTOTROPISM 2 (RPT2), the second founding member of the NRL family, appears

88   to play a role in sustaining phot1-NPH3 interactions at higher light intensities. RPT2 was first

89   identified from a genetic screen for mutants impaired in root phototropism (Okada and Shimura,

90   1992; Sakai et al., 2000) and is reported to interact with both phot1 and NPH3 (Inada et al., 2004;

91   Sullivan et al., 2009). Mutants that lack RPT2 exhibit normal phototropism to very low fluence

92   rates of unilateral blue light but show impaired curvature at higher light intensities (Haga et al.,

93   2015). Thus, RPT2 is believed to be important for promoting efficient phototropism under

94   brighter light conditions (Haga et al., 2015). This proposed function of RPT2 correlates well with

95   its expression profile, which increases upon irradiation in a fluence-rate dependent manner

96   (Inada et al., 2004; Tsuchida-Mayama et al., 2008; Haga et al., 2015). Nevertheless, how RPT2

97   functions alongside NPH3 to generate the lateral auxin gradient required for phototropic growth

98   remains poorly understood. The formation of this gradient appears to involve the activity of auxin

99   efflux carriers from both the PIN-FORMED (PIN) and ATP-BINDING CASSETTE B (ABCB) families

100   (Christie et al., 2011; Willige et al., 2013). PHYTOCHROME KINASE SUBSRTATE proteins (PKS1-4)

101   are also known to play a role in phototropism by influencing auxin transport or auxin-regulated

102   gene expression (Kami et al., 2014).

103   Phototropism in both mono- and dicotyledons has been studied extensively using dark-

104   grown (etiolated) seedlings (Christie and Murphy, 2013). Other photoreceptors, in addition to the

105   phots, modulate phototropic growth in etiolated seedlings when activated. For instance, the pre-

106   exposure of seedlings to red light accelerates the onset of phototropism in many plant species,

107   including in *Arabidopsis*, through the action of phytochrome A (phyA) (Sakai and Haga, 2012). This

108   effect of phyA on phototropism is restricted to low fluence rates of unilateral blue light and

109   appears to depend on signals that originate in tissues other than the epidermis (Kirchenbauer et

110   al., 2016; Sullivan et al., 2016). The study of phototropism in green (de-etiolated) seedlings has

111   received less attention by comparison (Christie and Murphy, 2013), but has gathered renewed

112   interest in recent years (Christie et al., 2011; Goyal et al., 2013; Hohm et al., 2014; Preuten et al.,

113   2015; Sullivan et al., 2016).

114   The aim of this study was to determine whether de-etiolation can modulate phototropic

115   responsiveness and to identify the underlying mechanism(s) by which this is achieved. Early work

116 has shown that the hypocotyl curvature responses of cress, lettuce, mustard, and radish are

117 enhanced in de-etiolated seedlings compared to etiolated seedlings (Hart and Macdonald, 1981;

118 Gordon et al., 1982). We now show that this also holds true for *Arabidopsis* and for other dicots,

119 and that this enhancement is underpinned by a molecular rheostat that fine-tunes the

120 phosphorylation status and subcellular localisation of NPH3, independently of the action of RPT2.

121

122 **Results**

123

124 **De-etiolation enhances the onset of phototropic growth**

125 Time-lapse imaging of free-standing seedlings germinated on a horizontal surface of moistened

126 silicon oxide provides a more reliable means to measure phototropic growth compared to

127 measurements that are conducted on seedlings grown on vertical agar plates (Sullivan et al.,

128 2016). We therefore used this approach to study the impact of de-etiolation on *Arabidopsis*

129 phototropism.

130   Etiolated seedlings were grown in darkness for 3 days prior to phototropic stimulation

131 with a low fluence rate of unilateral blue light (0.5 µmol m^{-2} s^{-1}). An identical growth regime was

132 used for de-etiolated seedlings, except that an 8-hour irradiation period with white light (80 µmol

133 m^{-2} s^{-1}) was introduced after 2 days of growth (Fig. 1A) Etiolated seedlings exhibited a lag time of

134 approximately 1 hour before a curvature response was observed (Fig. 1A). The onset of

135 phototropism in de-etiolated seedlings occurred more rapidly and was initiated within 30

136 minutes. Consequently, the curvature of de-etiolated seedlings reached saturation sooner than

137 in etiolated seedlings and at greater magnitude. A similar enhancement effect of de-etiolation on

138   phototropism was observed for tomato seedlings (Fig. S1). As reported previously (Christie et al.,

139   2011), the region of hypocotyl curvature is located more basally in de-etiolated seedlings

140   compared to etiolated seedlings (Fig. 1B). These differences coincide with the growth capacities

141   of etiolated and de-etiolated hypocotyls. For etiolated seedlings, the elongation zone resides

142   within the hypocotyl apex, whereas the largest growth capacity in de-etiolated seedlings is

143   located lower in the hypocotyl (Gendreau et al., 1997).

144

145   **De-etiolation by phytochrome or cryptochrome is sufficient to enhance phototropism**

146   Our examination of the *phot1* single mutant demonstrated that phot1 was responsible for

147   mediating hypocotyl phototropism to 0.5 µmol m^{-2} s^{-1} in both etiolated and de-etiolated seedlings

148   (Fig. 2A). Since phot2 protein levels are known to increase in response to irradiation (Christie and

149   Murphy, 2013), we rationalised that phot2 could be responsible for mediating the phototropic

150   enhancement in de-etiolated seedlings. Indeed, phot2 protein levels were higher in de-etiolated

151   versus etiolated seedlings, whereas the abundance of phot1 was reduced (Fig. S2). However,

152   mutants that lack phot2 still showed enhanced phototropism post greening (Fig. 2B), indicating

153   that phot2 is not required to mediate this process.

154   A brief (~15 min) pre-treatment with red or blue light is known to enhance the curvature

155   response of etiolated seedlings through the action of phyA (Kami et al., 2012; Sullivan et al., 2016).

156   We therefore examined whether de-etiolation under red or blue light was sufficient to enhance

157   phototropism. Our results showed that red, blue or white light were equally effective in

158   promoting phototropic enhancement (Fig. S3). Thus, we examined whether de-etiolation by phy

159   or cryptochrome (cry) blue-light receptors could enhance phototropism. Etiolated seedlings that

8

160   lack phyA and phyB exhibited a reduced phototropic response (Fig. 2C), compared to wild-type

161   seedlings (Fig. 1A). However, these results are consistent with previous reports that phyA is

162   necessary for the progression of normal phototropism in *Arabidopsis* (Whippo and Hangarter,

163   2004; Sullivan et al., 2016). De-etiolation was still able to elicit phototropic enhancement in the

164   *phyAphyB* mutant (Fig. 2C), indicating that this process is not solely dependent on the action of

165   phyA and phyB. Similar results were also obtained for *cry1cry2* mutants (Fig. 2D). Together, these

166   findings demonstrate that de-etiolation by either phytochrome or cryptochrome is sufficient to

167   enhance phototropism.

168

169   **De-etiolated hypocotyls do not exhibit increased sensitivity to auxin**

170   Lateral auxin accumulation on the shaded side of the hypocotyl is required to promote differential

171   cell elongation (Fankhauser and Christie, 2015). We therefore considered whether de-etiolated

172   seedlings exhibit a greater sensitivity to auxin. To determine this, we studied the impact of auxin

173   using a growth assay on hypocotyl sections, as reported previously (Takahashi et al., 2012).

174   Hypocotyl sections were isolated from etiolated and de-etiolated seedlings, using a red safe light,

175   and were placed onto agar medium and returned to darkness for 1-1.5 hours to deplete the

176   endogenous auxin pool. Consequently, little, if any, growth was subsequently detected in these

177   auxin-depleted hypocotyls (Fig. 3A, B). When these hypocotyl sections were transferred to a

178   medium containing the natural auxin, indole-3-actic acid (IAA), stem elongation occurred after a

179   lag time of ~10 minutes. Treatment with 10 or 100 µM IAA was equally effective at promoting

180   growth in both etiolated (Fig. 3A) and de-etiolated hypocotyls (Fig. 3B). However, de-etiolated

181   hypocotyls were notably less responsive to the IAA application and exhibited a lower degree of

182   auxin-induced elongation, compared to the etiolated hypocotyls. We therefore conclude that the

183   enhanced phototropic response of de-etiolated seedlings is not a consequence of increased

184   sensitivity to auxin. It is also reported that growth rate of etiolated seedlings is higher than that

185   of de-etiolated seedlings (Hart et al., 1982). Therefore, it is therefore unlikely that difference in

186   growth rates account for the enhanced phototropism in etiolated seedlings.

187

188   **De-etiolation alleviates NPH3 dephosphorylation**

189   We next examined whether aspects of phot1 signalling were altered in de-etiolated seedlings that

190   could account for the seedlings' enhanced responsiveness to light. NPH3 is an early signalling

191   component that plays a key role in establishing phototropic curvature (Liscum et al., 2014; Christie

192   et al., 2018). Phototropic measurements performed on the *nph3* mutant demonstrated that NPH3

193   is necessary to mediate hypocotyl curvature in both etiolated and de-etiolated seedlings (Fig. 4A).

194   The activation of phot1 leads to a rapid dephosphorylation of NPH3, which can be

195   detected by immunoblotting owing to its enhanced electrophoretic mobility (Fig. 4B). Light-

196   induced dephosphorylation was still apparent in de-etiolated seedlings but occurred to a much

197   lesser degree (Fig. 4B), with multiple phosphorylation products remaining over the 2-hour

198   irradiation period with 0.5 µmol m^{-2} s^{-1}. A similar effect on NPH3 dephosphorylation was also

199   observed in etiolated seedlings of the *pifq* mutant, which lacks the four PHYTOCHROME-

200   INTERACTING FACTORS (PIFs) PIF1, PIF3, PIF4 and PIF5 (Fig. 4D). This mutant is known to display

201   a constitutive photomorphogenic phenotype in darkness (Leivar et al., 2008) and is also impaired

202   in gravity sensing (Kim et al., 2011). Repositioning of *pifq* seedlings into a vertical position was

203   therefore necessary to assess their phototropic responsiveness. The phototropic response of

204   etiolated *pifq* seedlings was enhanced relative to wild-type etiolated seedlings (Fig. 4C). These

205   data provide further evidence that de-etiolation enhances the onset of phototropism by

206   diminishing NPH3 dephosphorylation. Further support for this conclusion comes from the

207   observation that reduced NPH3 dephosphorylation was evident in de-etiolated seedlings of

208   *phot2*, *phyAphyB* and *cry1cry2* mutants (Fig. 2E), which still showed enhanced phototropism upon

209   de-etiolation (Fig. 2B-D).

210   To discriminate whether the enhanced phototropism observed in etiolated *pifq* mutant

211   seedlings stems from reduced gravity sensing, we examined the phototropic responses of the

212   *pgm1* mutant which lacks PHOSPHOGLUCOMUTASE 1. Starchless mutants such as *pgm1* are

213   defective in gravity sensing and show enhanced root phototropism (Vitha et al., 2000). However,

214   phototropic enhancement was still apparent in *pgm1* mutants following de-etiolation (Fig. S4A),

215   as was reduced NPH3 dephosphorylation (Fig. S4B). These data therefore indicate that the impact

216   of de-etiolation on NPH3 phosphorylation status and phototropism does not depend on changes

217   in gravity sensing.

218

219   **De-etiolation reduces NPH3 aggregate formation**

220   Reduced dephosphorylation of NPH3 in response to de-etiolation was also apparent in transgenic

221   seedlings expressing NPH3 as a C-terminal translational fusion to GFP (Fig. S5), although the

222   electrophoretic mobility shift was less obvious in this line, presumably owing to the presence of

223   the GFP tag. *GFP-NPH3* expression in these lines was driven by the native *NPH3* promoter. GFP-

224   NPH3 was fully functional in restoring phototropism in the *nph3* mutant background, including

225   the phototropic enhancement in response to de-etiolation (Fig. S5).

226   GFP-NPH3 is primarily localised at the plasma membrane in darkness but is rapidly (within

227   minutes) internalised into aggregates upon blue light treatment (Mov. S1). The formation of these

228   aggregates depends on phot1 activity (Haga et al., 2015). Indeed, unilateral irradiation resulted

229   in differential NPH3 aggregate formation across the etiolated hypocotyl (Fig. 5). These findings

230   are in agreement with the proposal that a gradient of photoreceptor activation across the

231   hypocotyl is necessary to drive phototropic growth (Christie and Murphy, 2013). The difference

232   in GFP-NPH3 aggregate formation between the irradiated and the shaded side was more

233   significant in the upper hypocotyl than in the lower hypocotyl (Fig. 5), coinciding with this region

234   being the site of phototropic growth (Preuten et al., 2013; Yamamoto et al., 2014).

235   The kinetics for NPH3 dephosphorylation correlate closely with the timescale described

236   for the changes in NPH3 re-localisation (Haga et al., 2015). The treatment of etiolated hypocotyl

237   sections with the protein phosphatase inhibitor, okadaic acid (OKA), diminished the formation of

238   NPH3 aggregates (Fig. 6A). OKA treatment was equally effective in inhibiting the light-induced

239   dephosphorylation of NPH3 (Fig. S6). Thus, GFP aggregate formation is coupled to NPH3

240   dephosphorylation. With this in mind, we rationalised that de-etiolated seedlings, which retain a

241   sustained level of phosphorylated NPH3 following phototropic stimulation, should exhibit a

242   diminished GFP-NPH3 aggregate formation. Confocal microscopy confirmed that aggregate

243   formation is markedly reduced in de-etiolated seedlings, compared to etiolated seedlings (Fig.

244   6B).

245

246

247

248 **De-etiolation enhances phototropism by factors other than RPT2**

249 The NRL family member, RPT2, appears to play a role in sustaining phot1-NPH3 interactions at

250 higher light intensities and has been recently reported to have a role in modulating the

251 phosphorylation and localisation status of NPH3 (Haga et al., 2015). *RPT2* transcript abundance is

252 increased 20-fold in response to de-etiolation (Fig. S7). We therefore investigated whether RPT2

253 contributed to enhancing phototropism in de-etiolated seedlings. As reported previously (Haga

254 et al., 2015), etiolated seedlings of the *rpt2* mutant showed impaired hypocotyl phototropism at

255 0.5 µmol m^{-2} s^{-1} blue light (Fig. 7A). By contrast, de-etiolated *rpt2* seedlings exhibited a robust

256 response (Fig. 7A), indicating that RPT2 is not required for phototropism post de-etiolation.

257   The phototropic response of the *rpt2* mutant is indistinguishable from that of wild-type

258 etiolated seedlings at blue light intensities ≤ 0.01 µmol m^{-2} s^{-1} (Haga et al., 2015). At lower light

259 intensities (0.005 µmol m^{-2} s^{-1}), phototropic enhancement in response to de-etiolation was clearly

260 apparent in both wild-type seedlings (Fig. S8) and the *rpt2* mutant (Fig. 7B). Sustained levels of

261 NPH3 phosphorylation were also detected in de-etiolated seedlings of the *rpt2* mutant,

262 irrespective of whether 0.5 (Fig. 7C) or 0.005 µmol m^{-2} s^{-1} (Fig. 7D) was used for phototropic

263 stimulation. These findings demonstrate that the reduction in NPH3 dephosphorylation and the

264 promotion of phototropism in green seedlings occurs independently of RPT2.

265

266 **Reducing NPH3 dephosphorylation in etiolated seedlings enhances phototropism onset**

267 Since our findings suggest that NPH3's mode of action in initiating phototropism is fine-tuned by

268 modulating its phosphorylation status, we rationalised that if we could diminish NPH3

269 dephosphorylation in etiolated seedlings, we could potentially accelerate the onset of

270   phototropism. Etiolated seedlings were irradiated with 0.005, 0.5 and 20 µmol m^{-2} s^{-1} of unilateral

271   blue light for 1 hour and the phosphorylation status of NPH3 was examined by immunoblotting.

272   The dephosphorylation of NPH3 became more apparent as the light intensity increased (Fig. 8A).

273   In particular, NPH3 phosphorylation was substantially sustained at 0.005 µmol m^{-2} s^{-1}. Consistent

274   with a model in which reduced NPH3 dephosphorylation promotes phototropic responsiveness,

275   the onset of phototropism at 0.005 µmol m^{-2} s^{-1} was enhanced, compared to the response at 0.5

276   µmol m^{-2} s^{-1} (Fig. 8B). Conversely, phototropism was delayed at 20 µmol m^{-2} s^{-1} (Fig. 8B), which

277   corresponded to a small but detectable increase in NPH3 dephosphorylation (Fig. 8A).

278   In de-etiolated seedlings, NPH3 remained largely phosphorylated following irradiation

279   with 0.005 µmol m^{-2} s^{-1} (Fig. 8A). Phototropic responsiveness at this light was comparable to that

280   measured at 0.5 µmol m^{-2} s^{-1} (Fig. 8C). While there is a limit on how accurately we can measure

281   the phosphorylation status of NPH3 by immunoblotting, especially when multiple phosphorylated

282   forms of NPH3 appear to exist (Haga et al., 2015), irradiation at 20 µmol m^{-2} s^{-1} delayed the onset

283   of phototropism (Fig. 8C) and increased the level of NPH3 dephosphorylation (Fig. 8A). These data

284   therefore concur with a model in which maintaining a large pool of phosphorylated NPH3

285   promotes phototropic responsiveness, while maintaining a large pool of dephosphorylated NPH3

286   reduces phototropic responsiveness.

287

288   **Discussion**

289   Based on our findings, we propose that de-etiolation impacts the phosphorylation status and

290   subcellular localisation of NPH3, a core mediator of phototropic growth (Fig. 9). The regulation of

291   protein activity by protein phosphorylation is often viewed as being a binary switch. However,

292   our findings suggest that a finer rheostat-like process regulates NPH3; in this process, phototropic

293   responsiveness is altered by modulating the equilibrium that exists between different NPH3

294   phosphorylation states. Our observations that de-etiolation enhances phototropism in

295   Arabidopsis (Fig. 1) and tomato (Fig. S1) are consistent with earlier reports for other plant species

296   (Gordon et al., 1982; Hart et al., 1982; Ellis, 1987; Jin et al., 2001). Increased phototropic

297   responsiveness would enable de-etiolated seedlings to maximise their photoautrophic growth.

298   Etiolated seedlings transition from being heterotrophic to photoautotrophic as they undergo

299   phototropism. Indeed, a weaker phototropic response could help them to become established as

300   they emerge from the soil, before they acquire full photoautotrophic capacity.

301   The light-activation of phot1 triggers the rapid dephosphorylation of NPH3 (Fig. 4B),

302   whereas its re-phosphorylation can occur after a period of prolonged irradiation or when plants

303   are returned to darkness (Haga et al., 2015). The kinase(s) and phosphatase(s) responsible for this

304   regulation remain to be identified. However, we propose that the fine tuning of their activity

305   could alter the steady state levels of NPH3 phosphorylation, thereby altering the phototropic

306   response. This is especially apparent for de-etiolated seedlings, where a sustained level of NPH3

307   phosphorylation (Fig. 4B) underpins an enhanced phototropic response (Fig. 1A). A correlation

308   between a reduction in NPH3 dephosphorylation and an increase in phototropic responsiveness

309   was also detected in etiolated seedlings subjected to different intensities of phototropic

310   stimulation (Fig. 8). These findings lead us to conclude that sustained NPH3 phosphorylation and

311   plasma membrane localisation promotes its action in establishing hypocotyl curvature, whereas

312   NPH3 dephosphorylation and internalisation into aggregates diminishes it (Fig. 9). Such a model

313   is consistent with recent work showing that the re-phosphorylation of NPH3 is necessary for

314   sensory adaptation to promote efficient phototropism under brighter light conditions (Haga et

315   al., 2015; Christie et al., 2018). It is tempting to speculate that light-driven decreases in gibberellin

316   or brassinosteroid levels contribute to the enhancement effect of de-etiolation on phototropism.

317   However, gibberellin mutants exhibit reduced phototropism (Tsuchida-Mayama et al., 2010),

318   while brassinosteriod mutants show normal phototropism under the light conditions used in this

319   study (Whippo and Hangarter, 2005).

320   Multiple phosphorylation states of NPH3 appear to exist (Fig. 4B). Identifying the

321   differences between these phosphorylated forms and their functional significance will be

322   challenging. So far ~18 phosphorylation sites have been identified for NPH3 through global

323   phosphoproteomic approaches (Christie et al., 2018). Ser212, Ser222 and Ser236, which are

324   located downstream of the BTB domain, have been previously identified as being sites of

325   dephosphorylation (Tsuchida-Mayama et al., 2008). However, the mutation of these sites to

326   alanine does not appear to adversely affect the ability of NPH3 to mediate hypocotyl

327   phototropism in *Arabidopsis* (Tsuchida-Mayama et al., 2008; Haga et al., 2015). Further analysis

328   is therefore required to understand how phosphorylation impacts and influences the function of

329   NPH3.

330   Our current findings demonstrate that the dephosphorylation of NPH3 and its recruitment

331   into subcellular aggregates can be ameliorated by OKA, a potent inhibitor of PP1 and PP2A (Fig.

332   6B; Fig. S6). We therefore speculate that the sustained levels of NPH3 phosphorylation and

333   plasma membrane localisation, which correlate with the enhanced phototropic response of de-

334   etiolated seedlings, could arise from a reduced level of PP1/PP2A activity. While the treatment of

335   hypocotyl sections with OKA was successful in inhibiting NPH3 dephosphorylation, this was not

336   the case for intact seedlings (data not shown). It was therefore not possible to study the impact

337   of OKA treatment on phototropism using our experimental system. However, our genetic analysis

338   excludes the involvement of phot2 (Fig. 2B) and RPT2 (Fig. 7) in modulating the phosphorylation

339   status of NPH3 in de-etiolated seedlings. *RPT2* transcripts are abundant in de-etiolated seedlings

340   (Fig. S7), but the role of RPT2 in facilitating phototropism appears to negligible at blue light

341   intensities between 0.005-0.5 µmol m^{-2} s^{-1} (Fig.7B C). Recent work has shown that PKS4 acts in

342   conjunction with phot1 to reduce phototropic responsiveness at higher light intensities

343   (Schumacher et al., 2018). PKS4 is phosphorylated by phot1 (Demarsy et al., 2012), and the

344   accumulation of its phosphorylated form has been shown to delay phototropism (Schumacher et

345   al., 2018). However, this occurs by a mechanism that does not affect NPH3 dephosphorylation

346   (Schumacher et al., 2018).

347   NPH3 dephosphorylation is tissue- and, most likely, cell-autonomous (Sullivan et al.,

348   2016), which agrees with our observations that unilateral blue light can produce a gradient of

349   NPH3 aggregate formation across the irradiated hypocotyl (Fig. 5). Unilateral irradiation is

350   proposed to establish differential phot1 autophosphorylation across the oat coleoptile, with a

351   higher of level of phosphorylation occurring on the irradiated side (Salomon et al., 1997). The

352   subcellular aggregation profile of NPH3 within the seedling thus provides a convenient *in vivo*

353   reporter for phot1 kinase activity. The differential activation of phot1, brought about by unilateral

354   irradiation, leads auxin to accumulate on the shaded side of the hypocotyl (Christie et al., 2011;

355   Ding et al., 2011), where it promotes increased cell expansion. How this auxin gradient is

356   achieved, at a mechanistic level, remains unresolved. Mutants that lack the auxin efflux carriers

357   PIN3, PIN4 and PIN7, are severely compromised in phototropism (Willige et al., 2013). PIN3 is

358   laterally redistributed in etiolated seedlings following phototropic stimulation (Ding et al., 2011)

359   by a process that appears to be clathrin dependent (Zhang et al., 2017), but how its relocalisation

360   contributes to lateral auxin transport is still not known. PIN-mediated auxin transport is also

361   regulated by protein phosphorylation. D6 PROTEIN KINASES (D6PKs) are known to directly

362   phosphorylate PIN family members, and mutants deficient in D6PKs are defective in phototropism

363   (Willige et al., 2013). Yet, how such changes in phosphorylation coordinate with phot1 and NPH3

364   remain poorly understood.

365   Phot1-NPH3 interactions at the plasma membrane are transiently disrupted upon

366   irradiation (Haga et al., 2015), consistent with the partial re-localisation of these proteins to

367   different subcellular regions; phot1 internalises into cytosolic structures (Sakamoto and Briggs,

368   2002), whereas NPH3 accumulates in subcellular aggregates (Mov. S1). The functional relevance

369   of these transient changes in subcellular localisation are still not known. At least for phot1,

370   approaches aimed at tethering the photoreceptor to the plasma membrane through lipid binding

371   suggest that diminishing its light-induced internalisation does not alter its ability to function in

372   *Arabidopsis* (Preuten et al., 2015). Moreover, biochemical fractionation experiments indicate that

373   NPH3 aggregates accumulate in the cytosol (Haga et al., 2015) and that their formation is

374   unaffected by cytoskeleton inhibitors or by inhibitors of vesicle trafficking (Haga et al., 2015).

375   Although the identity of these aggregates has not been determined, their occurrence is highly

376   dynamic (Mov. S1).

377   It is worth noting that the N- and C-terminal regions of NPH3 are predicted to be

378   disordered (Fig. S9). Intrinsically disordered regions (IDRs) within proteins are increasing

379   recognised as being important determinants of cellular signalling (Wright and Dyson, 2015) and

380   can offer accessibility for assembling protein complexes. IDRs are often regions that are targeted

381   for post-translational modification (Bah and Forman-Kay, 2016) and are associated with the

382   dynamic self-assembly of membrane-less nuclear or cytosolic organelles (Cuevas-Velazquez and

383   Dinneny, 2018). Thus, the phosphorylation-dependent modulation of IDRs within NPH3 could

384   produce different signalling outputs via alterations in its subcellular localisation and in its affinity

385   for its interaction partners.

386   NPH3 has been identified as being a component of the 14-3-3 interactome in barley

387   (Schoonheim et al., 2007). 14-3-3 proteins are also known to bind to phot1 and phot2 upon

388   receptor autophosphorylation (Inoue et al., 2008; Sullivan et al., 2009; Tseng et al., 2012) but the

389   functional relevance of this interaction remains unknown. Further studies are now required to

390   evaluate how 14-3-3 binding integrates into the rheostat-like mechanism that we propose from

391   the present findings governs the phosphorylation and subcellular localisation status of NPH3 (Fig.

392   9).

393

394   **Materials and Methods**

395

396   **Plant material and growth**

397   Wild-type (*gl-1*, ecotype Columbia), *phot1-5* (Liscum and Briggs, 1995), *phot2-1* (Kagawa et al.,

398   2001), *phyA-211 phyB-9* (Sullivan et al., 2016), *cry1-304 cry2-1* (Mockler et al., 1999), *nph3-6*

399   (Motchoulski and Liscum, 1999), *rpt2-2* (Inada et al., 2004) and the *pif1 pif3 pif4 pif5* quadruple

400   mutant (*pifq*) (Leivar et al., 2008) were previously described. Seeds were surface sterilised and

401   planted on half-strength Murashige and Skoog (MS) medium with 0.8% agar (w/v) and grown

402   vertically or sown in transparent plastic entomology boxes (Watkins and Doncaster) on a layer of

403   silicon dioxide (Sigma-Aldrich) watered with quarter-strength MS medium. Following

404   stratification in the dark at 4°C for 2-5 days, seeds were exposed to 80 µmol m^{-2} s^{-1} white light for

405   6-8 h to induce germination before incubation in the dark for 64 h for etiolated seedlings. De-

406   etiolated seedlings were incubated in the dark for 40 h, exposed to 80 µmol m^{-2} s^{-1} white light for

407   8 h, and then dark-adapted for 16 h. For red or blue light treatments, white fluorescent light was

408   filtered through Deep Golden Amber filter No. 135 (Lee Filters) or Moonlight Blue filter No. 183

409   (Lee Filters), respectively. Fluence rates for all light sources were measured with a Li-250A and

410   quantum sensor (LI-COR).

411

412   **Transformation of *Arabidopsis***

413   The transformation vector for *NPH3::GFP-NPH3* was constructed using the modified binary

414   expression vector pEZR(K)-LC (Christie et al., 2002). The *35S* promoter was removed using

415   restriction sites *SacI* and *HindIII* and replaced with the 2.1 kb *NPH3* promoter amplified from

416   Columbia genomic DNA with primers pNPH3-F (5'-

417   AAAAGAGCTCAAACCCCACATTAATCAGACAGAATC -3') and pNPH3-R (5'-

418   AAAAAAGCTTACACAAGTTAACACTCTCTGTAGTTG -3'). The full-length coding sequence of *NPH3*

419   was amplified from cDNA and inserted using restriction sites *KpnI* and *BamHI*. The *nph3-6* mutant

420   was transformed with *Agrobacterium tumefaciens* strain GV3101, as previously described (Davis

421   et al., 2009). Based on the segregation of kanamycin resistance, independent homozygous T3

422   lines were selected for analysis.

423

Phototropism

Phototropism of 3-day-old etiolated and de-etiolated seedlings grown on a layer of silicon dioxide was performed, as previously described (Sullivan et al., 2016). Images of seedlings were captured every 10 min for 4 h, or every 20 min for 8 h, during unilateral illumination with 0.5 μmol m^{-2} s^{-1} or 0.005 μmol m^{-2} s^{-1} of blue light with a Retiga 6000 CCD camera (QImaging), connected to a PC running QCapture Pro 7 software (QImaging) with supplemental infrared LED illumination. Measurements of hypocotyl angles were made using Fiji software (Schindelin et al., 2012). Tomato seeds (*Solanum lycopersicum* var Ailsa Craig) were germinated on wet filter paper in the dark for 3days at 25°C ± 2°C. Single, germinated seeds were transferred into custom growth discs (3 cm x 1.5 cm), which contained a mixture of organic potting garden soil mix (Pepper Agro, Bangalore, India) and peat (1:3), and were grown for an additional 72 h in the dark for etiolated seedlings. De-etiolated seedlings were incubated in the dark for 48 h, exposed to 10 μmol m^{-2} s^{-1} white light for 8 h and then dark-adapted for 16 h. The seedlings were irradiated with 0.5 μmol m^{-2} s^{-1} blue light obtained from blue (λ_{max}470) light-emitting diodes (Kwality Photonics, Hyderabad, India). Images were captured every 10 min for 2 h with a C270 HD camera (Logitech) connected to a PC running Chronolapse software (http://code.google.com/p/chronolapse/) and supplemented with infra-red illumination. Measurements of hypocotyl angles were performed using NIH ImageJ software.

Immunoblot analysis

Total proteins were extracted from 3-day-old etiolated or de-etiolated seedlings by directly grinding 50 seedlings in 100 μl of 2 X SDS sample buffer under red safe light illumination. Proteins

446   were transferred onto polyvinylidene fluoride membrane (Bio-Rad) with a Trans-Blot Turbo

447   Transfer System (Bio-Rad) and detected with anti-phot1 or anti-phot2 polyclonal antibodies (Cho

448   et al., 2007), anti-NPH3 polyclonal antibody (Tsuchida-Mayama et al., 2008) and anti-UGPase

449   polyclonal antibody (Agrisera). Blots were developed with horseradish peroxidase-linked

450   secondary antibodies (Promega) and Pierce ECL Plus Western Blotting Substrate (Thermo Fisher

451   Scientific).

452

453   **Confocal microscopy**

454   Localization of GFP-tagged NPH3 was visualized using a Leica SP8 laser scanning confocal

455   microscope. The 488 nm excitation line was used and GFP fluorescence collected between 505-

456   530 nm. Images were acquired at 1024 x 1024-pixel resolution with a line average of two. To

457   image etiolated seedlings following unilateral irradiation, seedlings were transferred onto

458   microscope slides covered with a thin layer of half-strength MS medium with 0.8% agar (w/v).

459   Seedlings were maintained in darkness or irradiated with unilateral blue light for 1 h before two

460   partially overlapping sets of images were acquired. Images were assembled by using the Pairwise

461   Stitching Plugin for Fiji (Preibisch et al., 2009). The number of GFP particles was measured using

462   the Analyze Particles tool of Fiji, with a diameter of 0.5-50 µm and circularity of 0.5-1.0.

463

464   **Okadaic acid treatment**

465   Okadaic acid (OKA; Abcam) was prepared as a 1 mM stock solution in dimethyl sulfoxide (DMSO).

466   Hypocotyl segments of etiolated and de-etiolated seedlings were prepared by dissection

467   immediately below the cotyledonary node and root-shoot junction, under a dissecting

22

468   microscope with micro scissors (Fine Science Tools, Germany) using red safe light illumination.

469   Dissected seedlings were transferred to 6-well plates containing quarter-strength MS medium

470   and the indicated concentration of OKA or DMSO as solvent control; the final DMSO

471   concentration was 1 % (v/v) for all treatments. Seedlings were vacuum infiltrated for 15 min,

472   followed by incubation in darkness for 2 h with gentle agitation. Seedlings were maintained in

473   darkness or irradiated with the indicated fluence of blue light for 1 h before confocal observation

474   or protein extraction. For protein extraction, seedlings were blotted on filter paper before

475   undergoing grinding in 2 X SDS sample buffer.

476

477   **Hypocotyl elongation assay**

478   Hypocotyl elongation assays were performed according to (Takahashi et al., 2012). Apical

479   hypocotyl segments of 4 mm were prepared from etiolated or de-etiolated seedlings under a

480   dissecting microscope with micro scissors (Fine Science Tools, Germany) and incubated on

481   depletion media (10 mM KCl, 1 mM MES- KOH [pH 6.0], 0.8% agar) for 1 to 1.5 h in darkness.

482   Hypocotyl segments were transferred to depletion media that contained 0, 10 or 100 µM

483   indoleacetic acid (IAA) and were photographed with a digital camera every 10 min, for 90 min. All

484   manipulations were performed under red safe light illumination. Hypocotyl segment lengths were

485   measured using Fiji software (Schindelin et al., 2012).

486

487   **Transcript analysis**

488   Total RNA was isolated from 3-day-old etiolated and de-etiolated seedlings using the RNeasy

489   Plant Mini Kit (Qiagen) and was DNase treated (Turbo DNA- free; Thermo Fisher Scientific).

490   Complementary DNA (cDNA) was synthesised from 1 μg of total RNA using oligo dT and

491   SuperScript II reverse transcriptase (Thermo Fisher Scientific). qPCR reactions were performed

492   with Brilliant III SYBR Green QPCR Master Mix (Agilent) on a StepOnePlus (Thermo Fisher

493   Scientific) real-time PCR system using primers for RPT2 (RTP2-F, 5'-

494   TTGCTGGTCGGACACAAGACTTC -3'; RTP2-R, 5'- CATTGCCTCGTTGCAAGCCTTAG-3'). IRON SULFUR

495   CLUSTER ASSEMBLY PROTEIN 1 (ISU1, AT4G22220) was used as the reference gene (Bordage et

496   al., 2016).

497

498   **Protein Disorder Prediction**

499   Protein disorder was predicted by using the online server PrDOS (Ishida and Kinoshita, 2007).

500

508

509   **Author Contributions**

510   J.M.C., S.S. designed and directed the research. S.S. planned and performed experiments. J.L.

511   performed transcript analysis, whereas E.K. performed phototropic experiments in tomato

512   seedlings. T.S. provided reagents. J.M.C., S.S. analysed the data and wrote the manuscript. All

513   authors commented on the manuscript.

514

515   **Supplementary Figure S1.** De-etiolated tomato seedlings show enhanced kinetics of

516   phototropism.

517

518   **Supplementary Figure S2.** Protein abundance of phot1 and phot2 in etiolated and de-etiolated

519   seedlings.

520

521   **Supplementary Figure S3.** Phototropic response of wild-type seedlings de-etiolated under

522   different light conditions.

523

524   **Supplementary Figure S4.** Phototropic responses and NPH3 phosphorylation status in etiolated

525   and de-etiolated seedlings of the *pgm1* mutant.

526

527   **Supplementary Figure S5.** GFP-NPH3 functionality and phosphorylation status in etiolated and

528   de-etiolated seedlings.

529

530   **Supplementary Figure S6.** Effect of OKA treatment on blue light-induced NPH3

531   dephosphorylation.

532

533

534   **Supplementary Figure S7.** De-etiolated seedlings have increased *RPT2* expression levels.

535

536   **Supplementary Figure S8.** De-etiolated wild-type seedlings show enhanced phototropism at

537   0.005 µmol m^{-2} s^{-1} of unliteral blue light.

538

539   **Supplementary Figure S9.** PrDOS plot of disordered regions in NPH3.

540

541   **Supplementary Movie S1.** Dynamic blue light-induced changes in the subcellular localisation of

542   GFP-NPH3.

543

544   **References**

545   **Bah A, Forman-Kay JD** (2016) Modulation of Intrinsically Disordered Protein Function by Post-
546   translational Modifications. Journal of Biological Chemistry **291:** 6696-6705
547   **Bordage S, Sullivan S, Laird J, Millar AJ, Nimmo HG** (2016) Organ specificity in the plant circadian
548   system is explained by different light inputs to the shoot and root clocks. New Phytologist
549   **212:** 136-149
550   **Cho HY, Tseng TS, Kaiserli E, Sullivan S, Christie JM, Briggs WR** (2007) Physiological roles of the
551   light, oxygen, or voltage domains of phototropin 1 and phototropin 2 in Arabidopsis. Plant
552   Physiol **143:** 517-529
553   **Christie JM, Murphy AS** (2013) Shoot phototropism in higher plants: new light through old
554   concepts. Am J Bot **100:** 35-46
555   **Christie JM, Suetsugu N, Sullivan S, Wada M** (2018) Shining Light on the Function of NPH3/RPT2-
556   Like Proteins in Phototropin Signaling. Plant Physiol **176:** 1015-1024
557   **Christie JM, Swartz TE, Bogomolni RA, Briggs WR** (2002) Phototropin LOV domains exhibit
558   distinct roles in regulating photoreceptor function. Plant J **32:** 205-219
559   **Christie JM, Yang H, Richter GL, Sullivan S, Thomson CE, Lin J, Titapiwatanakun B, Ennis M,**
560   **Kaiserli E, Lee OR, Adamec J, Peer WA, Murphy AS** (2011) phot1 inhibition of ABCB19
561   primes lateral auxin fluxes in the shoot apex required for phototropism. PLoS Biol **9:**
562   e1001076
563   **Cuevas-Velazquez CL, Dinneny JR** (2018) Organization out of disorder: liquid-liquid phase
564   separation in plants. Curr Opin Plant Biol **45:** 68-74

565 **Davis AM, Hall A, Millar AJ, Darrah C, Davis SJ** (2009) Protocol: Streamlined sub-protocols for
566 floral-dip transformation and selection of transformants in Arabidopsis thaliana. Plant
567 Methods **5:** 3
568 **Demarsy E, Schepens I, Okajima K, Hersch M, Bergmann S, Christie J, Shimazaki K, Tokutomi S,**
569 **Fankhauser C** (2012) Phytochrome Kinase Substrate 4 is phosphorylated by the
570 phototropin 1 photoreceptor. EMBO J **31:** 3457-3467
571 **Deng Z, Oses-Prieto JA, Kutschera U, Tseng TS, Hao L, Burlingame AL, Wang ZY, Briggs WR** (2014)
572 Blue light-induced proteomic changes in etiolated Arabidopsis seedlings. J Proteome Res
573 **13:** 2524-2533
574 **Ding Z, Galvan-Ampudia CS, Demarsy E, Langowski L, Kleine-Vehn J, Fan Y, Morita MT, Tasaka**
575 **M, Fankhauser C, Offringa R, Friml J** (2011) Light-mediated polarization of the PIN3 auxin
576 transporter for the phototropic response in Arabidopsis. Nat Cell Biol **13:** 447-452
577 **Ellis RJ** (1987) Comparison of Fluence-Response Relationships of Phototropism in Light-Grown
578 and Dark-Grown Buckwheat. Plant Physiology **85:** 689-692
579 **Fankhauser C, Christie JM** (2015) Plant phototropic growth. Curr Biol **25:** R384-389
580 **Gendreau E, Traas J, Desnos T, Grandjean O, Caboche M, Hofte H** (1997) Cellular basis of
581 hypocotyl growth in Arabidopsis thaliana. Plant Physiology **114:** 295-305
582 **Gordon DC, Macdonald IR, Hart JW** (1982) Regional Growth-Patterns in the Hypocotyls of
583 Etiolated and Green Cress Seedlings in Light and Darkness. Plant Cell and Environment **5:**
584 347-353
585 **Goyal A, Szarzynska B, Fankhauser C** (2013) Phototropism: at the crossroads of light-signaling
586 pathways. Trends Plant Sci **18:** 393-401
587 **Haga K, Takano M, Neumann R, Iino M** (2005) The Rice COLEOPTILE PHOTOTROPISM1 gene
588 encoding an ortholog of Arabidopsis NPH3 is required for phototropism of coleoptiles and
589 lateral translocation of auxin. Plant Cell **17:** 103-115
590 **Haga K, Tsuchida-Mayama T, Yamada M, Sakai T** (2015) Arabidopsis ROOT PHOTOTROPISM2
591 Contributes to the Adaptation to High-Intensity Light in Phototropic Responses. Plant Cell
592 **27:** 1098-1112
593 **Hart JW, Gordon DC, Macdonald IR** (1982) Analysis of Growth during Phototropic Curvature of
594 Cress Hypocotyls. Plant Cell and Environment **5:** 361-366
595 **Hart JW, Macdonald IR** (1981) Phototropic Responses of Hypocotyls of Etiolated and Green
596 Seedlings. Plant Science Letters **21:** 151-158
597 **Hohm T, Demarsy E, Quan C, Allenbach Petrolati L, Preuten T, Vernoux T, Bergmann S,**
598 **Fankhauser C** (2014) Plasma membrane H(+) -ATPase regulation is required for auxin
599 gradient formation preceding phototropic growth. Mol Syst Biol **10:** 751
600 **Inada S, Ohgishi M, Mayama T, Okada K, Sakai T** (2004) RPT2 is a signal transducer involved in
601 phototropic response and stomatal opening by association with phototropin 1 in
602 Arabidopsis thaliana. Plant Cell **16:** 887-896
603 **Inoue S, Kinoshita T, Matsumoto M, Nakayama KI, Doi M, Shimazaki K** (2008) Blue light-induced
604 autophosphorylation of phototropin is a primary step for signaling. Proc Natl Acad Sci U S
605 A **105:** 5626-5631
606 **Inoue S, Kinoshita T, Takemiya A, Doi M, Shimazaki K** (2008) Leaf positioning of Arabidopsis in
607 response to blue light. Mol Plant **1:** 15-26

608 **Ishida T, Kinoshita K** (2007) PrDOS: prediction of disordered protein regions from amino acid
609   sequence. Nucleic Acids Res **35:** W460-464

610 **Jin X, Zhu J, Zeiger E** (2001) The hypocotyl chloroplast plays a role in phototropic bending of
611   Arabidopsis seedlings: developmental and genetic evidence. Journal of Experimental
612   Botany **52:** 91-97

613 **Kagawa T, Sakai T, Suetsugu N, Oikawa K, Ishiguro S, Kato T, Tabata S, Okada K, Wada M** (2001)
614   Arabidopsis NPL1: a phototropin homolog controlling the chloroplast high-light avoidance
615   response. Science **291:** 2138-2141

616 **Kami C, Allenbach L, Zourelidou M, Ljung K, Schutz F, Isono E, Watahiki MK, Yamamoto KT,**
617   **Schwechheimer C, Fankhauser C** (2014) Reduced phototropism in pks mutants may be
618   due to altered auxin-regulated gene expression or reduced lateral auxin transport. Plant J
619   **77:** 393-403

620 **Kami C, Hersch M, Trevisan M, Genoud T, Hiltbrunner A, Bergmann S, Fankhauser C** (2012)
621   Nuclear phytochrome A signaling promotes phototropism in Arabidopsis. Plant Cell **24:**
622   566-576

623 **Kim K, Shin J, Lee SH, Kweon HS, Maloof JN, Choi G** (2011) Phytochromes inhibit hypocotyl
624   negative gravitropism by regulating the development of endodermal amyloplasts through
625   phytochrome-interacting factors. Proceedings of the National Academy of Sciences of the
626   United States of America **108:** 1729-1734

627 **Kirchenbauer D, Viczian A, Adam E, Hegedus Z, Klose C, Leppert M, Hiltbrunner A, Kircher S,**
628   **Schafer E, Nagy F** (2016) Characterization of photomorphogenic responses and signaling
629   cascades controlled by phytochrome-A expressed in different tissues. New Phytol **211:**
630   584-598

631 **Leivar P, Monte E, Oka Y, Liu T, Carle C, Castillon A, Huq E, Quail PH** (2008) Multiple
632   Phytochrome-Interacting bHLH Transcription Factors Repress Premature Seedling
633   Photomorphogenesis in Darkness. Current Biology **18:** 1815-1823

634 **Liscum E, Askinosie SK, Leuchtman DL, Morrow J, Willenburg KT, Coats DR** (2014) Phototropism:
635   growing towards an understanding of plant movement. Plant Cell **26:** 38-55

636 **Liscum E, Briggs WR** (1995) Mutations in the NPH1 locus of Arabidopsis disrupt the perception of
637   phototropic stimuli. Plant Cell **7:** 473-485

638 **Mockler TC, Guo HW, Yang HY, Duong H, Lin CT** (1999) Antagonistic actions of Arabidopsis
639   cryptochromes and phytochrome B in the regulation of floral induction. Development **126:**
640   2073-2082

641 **Motchoulski A, Liscum E** (1999) Arabidopsis NPH3: A NPH1 photoreceptor-interacting protein
642   essential for phototropism. Science **286:** 961-964

643 **Okada K, Shimura Y** (1992) Mutational analysis of root gravitropism and phototropism of
644   Arabidopsis thaliana seedlings. Australian Journal of Plant Physiology **19:** 439-448

645 **Pedmale UV, Liscum E** (2007) Regulation of phototropic signaling in Arabidopsis via
646   phosphorylation state changes in the phototropin 1-interacting protein NPH3. J Biol Chem
647   **282:** 19992-20001

648 **Preibisch S, Saalfeld S, Tomancak P** (2009) Globally optimal stitching of tiled 3D microscopic
649   image acquisitions. Bioinformatics **25:** 1463-1465

650   **Preuten T, Blackwood L, Christie JM, Fankhauser C** (2015) Lipid anchoring of Arabidopsis
651   phototropin 1 to assess the functional significance of receptor internalization: should I
652   stay or should I go? New Phytol **206:** 1038-1050
653   **Preuten T, Hohm T, Bergmann S, Fankhauser C** (2013) Defining the site of light perception and
654   initiation of phototropism in Arabidopsis. Curr Biol **23:** 1934-1938
655   **Roberts D, Pedmale UV, Morrow J, Sachdev S, Lechner E, Tang X, Zheng N, Hannink M, Genschik**
656   **P, Liscum E** (2011) Modulation of phototropic responsiveness in Arabidopsis through
657   ubiquitination of phototropin 1 by the CUL3-Ring E3 ubiquitin ligase CRL3(NPH3). Plant
658   Cell **23:** 3627-3640
659   **Sakai T, Haga K** (2012) Molecular genetic analysis of phototropism in Arabidopsis. Plant Cell
660   Physiol **53:** 1517-1534
661   **Sakai T, Kagawa T, Kasahara M, Swartz TE, Christie JM, Briggs WR, Wada M, Okada K** (2001)
662   Arabidopsis nph1 and npl1: blue light receptors that mediate both phototropism and
663   chloroplast relocation. Proc Natl Acad Sci U S A **98:** 6969-6974
664   **Sakai T, Wada T, Ishiguro S, Okada K** (2000) RPT2. A signal transducer of the phototropic response
665   in Arabidopsis. Plant Cell **12:** 225-236
666   **Sakamoto K, Briggs WR** (2002) Cellular and subcellular localization of phototropin 1. Plant Cell
667   **14:** 1723-1735
668   **Salomon M, Zacherl M, Rudiger W** (1997) Asymmetric, blue light-dependent phosphorylation of
669   a 116-kilodalton plasma membrane protein can be correlated with the first- and second-
670   positive phototropic curvature of oat coleoptiles. Plant Physiol **115:** 485-491
671   **Schindelin J, Arganda-Carreras I, Frise E, Kaynig V, Longair M, Pietzsch T, Preibisch S, Rueden C,**
672   **Saalfeld S, Schmid B, Tinevez JY, White DJ, Hartenstein V, Eliceiri K, Tomancak P, Cardona**
673   **A** (2012) Fiji: an open-source platform for biological-image analysis. Nature Methods **9:**
674   676-682
675   **Schoonheim PJ, Veiga H, Pereira DD, Friso G, van Wijk KJ, de Boer AH** (2007) A comprehensive
676   analysis of the 14-3-3 interactome in barley leaves using a complementary proteomics and
677   two-hybrid approach. Plant Physiology **143:** 670-683
678   **Schumacher P, Demarsy E, Waridel P, Petrolati LA, Trevisan M, Fankhauser C** (2018) A
679   phosphorylation switch turns a positive regulator of phototropism into an inhibitor of the
680   process. Nature Communications **9**
681   **Sullivan S, Hart JE, Rasch P, Walker CH, Christie JM** (2016) Phytochrome A Mediates Blue-Light
682   Enhancement of Second-Positive Phototropism in Arabidopsis. Front Plant Sci **7:** 290
683   **Sullivan S, Takemiya A, Kharshiing E, Cloix C, Shimazaki KI, Christie JM** (2016) Functional
684   characterization of Arabidopsis phototropin 1 in the hypocotyl apex. Plant J **88:** 907-920
685   **Sullivan S, Thomson CE, Kaiserli E, Christie JM** (2009) Interaction specificity of Arabidopsis 14-3-
686   3 proteins with phototropin receptor kinases. FEBS Lett **583:** 2187-2193
687   **Takahashi K, Hayashi K, Kinoshita T** (2012) Auxin Activates the Plasma Membrane H+-ATPase by
688   Phosphorylation during Hypocotyl Elongation in Arabidopsis. Plant Physiology **159:** 632-+
689   **Tseng TS, Whippo C, Hangarter RP, Briggs WR** (2012) The role of a 14-3-3 protein in stomatal
690   opening mediated by PHOT2 in Arabidopsis. Plant Cell **24:** 1114-1126
691   **Tsuchida-Mayama T, Nakano M, Uehara Y, Sano M, Fujisawa N, Okada K, Sakai T** (2008) Mapping
692   of the phosphorylation sites on the phototropic signal transducer, NPH3. Plant Science**:**
693   626-633

694 **Tsuchida-Mayama T, Sakai T, Hanada A, Uehara Y, Asami T, Yamaguchi S** (2010) Role of the
695   phytochrome and cryptochrome signaling pathways in hypocotyl phototropism. Plant J
696   **62:** 653-662
697 **Vitha S, Zhao L, Sack FD** (2000) Interaction of root gravitropism and phototropism in Arabidopsis
698   wild-type and starchless mutants. Plant Physiol **122:** 453-462
699 **Whippo C, Hangarter R** (2004) Phytochrome modulation of blue-light-induced
700 phototropism. Plant Cell Environ **27:** 1223-1228
701 **Whippo CW, Hangarter RP** (2005) A brassinosteroid-hypersensitive mutant of BAK1 indicates that
702   a convergence of photomorphogenic and hormonal signaling modulates phototropism.
703   Plant Physiol **139:** 448-457
704 **Willige BC, Ahlers S, Zourelidou M, Barbosa IC, Demarsy E, Trevisan M, Davis PA, Roelfsema MR,**
705   **Hangarter R, Fankhauser C, Schwechheimer C** (2013) D6PK AGCVIII kinases are required
706   for auxin transport and phototropic hypocotyl bending in Arabidopsis. Plant Cell **25:** 1674-
707   1688
708 **Wright PE, Dyson HJ** (2015) Intrinsically disordered proteins in cellular signalling and regulation.
709   Nature Reviews Molecular Cell Biology **16:** 18-29
710 **Yamamoto K, Suzuki T, Aihara Y, Haga K, Sakai T, Nagatani A** (2014) The phototropic response is
711   locally regulated within the topmost light-responsive region of the Arabidopsis thaliana
712   seedling. Plant Cell Physiol **55:** 497-506
713 **Zhang Y, Yu QQ, Jiang N, Yan X, Wang C, Wang QM, Liu JZ, Zhu MY, Bednarek SY, Xu J, Pan JW**
714   (2017) Clathrin regulates blue light-triggered lateral auxin distribution and hypocotyl
715   phototropism in Arabidopsis. Plant Cell and Environment **40:** 165-176
716

717 **Figure legends**

718 **Figure 1.** De-etiolation enhances phototropism and alters the position of hypocotyl curvature.

719 **(A)** Experimental design for analysing phototropism in etiolated and de-etiolated seedlings (top).

720 Etiolated seedlings were grown in darkness for 3 days. For de-etiolated seedlings, de-etiolation

721 was induced in 2-day-old, dark-grown seedlings, with an 8 h white-light treatment (80 µmol m^{-2}

722 s^{-1}), followed by a 16 h dark-adaptation. 3-day-old etiolated and de-etiolated seedlings were

723 placed into unilateral blue light to analyse hypocotyl phototropism. Phototropism of etiolated

724 and de-etiolated seedlings irradiated with 0.5 µmol m^{-2} s^{-1} of unliteral blue light (bottom).

725 Hypocotyl curvatures were measured every 10 min for 4 h, and each value is the mean ± S.E. of

726 20 seedlings. **(B)** Position of hypocotyl curvature in etiolated (Et) and de-etiolated (De-et) wild-

727   type seedlings (top). Composite image of etiolated (left) and de-etiolated (right) seedling at 0, 20,

728   40 and 60 min after commencement of curvature. Arrows indicate position of hypocotyl

729   curvature. Quantification of the position of hypocotyl curvature (bottom), as measured from the

730   base of the hypocotyl (with 0 being the closest, and 1 the farthest). The recorded position was

731   divided by total hypocotyl length to give the relative position of curvature. Values are the mean

732   ± S.E. of 20 seedlings.

733

734   **Figure 2.** Phototropic responses and NPH3 phosphorylation status in etiolated and de-etiolated

735   seedlings of photoreceptor mutants.

736   Phototropism of etiolated and de-etiolated *phot1* **(A)** *phot2* **(B)** *phyAphyB* **(C)** and *cry1cry2* **(D)**

737   mutant seedlings, irradiated with 0.5 µmol m^{-2} s^{-1} of unilateral blue light. Hypocotyl curvatures

738   were measured every 10 min for 4 h, and each value is the mean ± S.E. of 17-20 seedlings. **(E)**

739   Immunoblot analysis of total protein extracts from etiolated (Et) and de-etiolated (De-et) *phot1*,

740   *phot2*, *phyAphyB* and *cry1cry2* mutant seedlings, maintained in darkness (D) or irradiated with

741   0.5 µmol m^{-2} s^{-1} of unilateral blue light for 60 min (L). Protein extracts were probed with anti-

742   NPH3 antibody.

743

744   **Figure 3.** Auxin-induced elongation of hypocotyl segments of etiolated and de-etiolated seedlings.

745   Elongation of 4 mm apical hypocotyl segments prepared from etiolated **(A)** or de-etiolated **(B)**

746   seedlings. Hypocotyl segments were placed on media containing 0, 10 or 100 µM IAA, and

747   hypocotyl segment lengths were measured every 10 min for 90 min. Each value is the mean ± S.E.

748   of 30 seedlings.

749

Figure 4. NPH3 functionality and phosphorylation status in etiolated and de-etiolated seedlings.

(A) Phototropism of etiolated and de-etiolated *nph3* mutant seedlings irradiated with 0.5 µmol

$m^{-2}\,s^{-1}$ of unliteral blue light. Hypocotyl curvatures were measured every 10 min for 4 h and each

value is the mean ± S.E. of 20 seedlings. **(B)** NPH3 phosphorylation status in etiolated and de-

etiolated seedlings during irradiation with blue light . Immunoblot analysis of total protein

extracts from etiolated and de-etiolated wild-type seedlings maintained in darkness (D) or

irradiated with 0.5 µmol $m^{-2}\,s^{-1}$ of unilateral blue light for 5, 15, 30, 60 or 120 min. Protein extracts

were probed with anti-NPH3 antibody. **(C)** Phototropism of etiolated *pifq* mutant seedlings

irradiated with 0.5 µmol $m^{-2}\,s^{-1}$ of unliteral blue light. Hypocotyl curvatures were measured every

10 min for 4 h and each value is the mean ± S.E. of 20 seedlings. Phototropic responses of etiolated

and d-etiolated wild-type (WT) seedlings are also shown. **(D)** Immunoblot analysis of total protein

extracts from etiolated wild-type (WT), *pif1 pif3 pif4 pif5* (*pifq*) quadruple mutant, and

phot1phot2 (p1p2) double mutant seedlings maintained in darkness (D) or irradiated with 0.5

µmol $m^{-2}\,s^{-1}$ of unilateral blue light for 60 min (L). Protein extracts were probed with anti-NPH3

antibody.

765

Figure 5. Effect of unilateral blue light irradiation on GFP-NPH3 localisation across the hypocotyl.

(A) Confocal images of etiolated *NPH3::GFP-NPH3#1* seedlings maintained in (left) darkness or

(right) irradiated with 0.5 µmol $m^{-2}\,s^{-1}$ of unilateral blue light for 60 min,. Arrows indicate the

direction of blue light. Hypocotyl images were divided into irradiated and shaded sides, and then

into upper and lower halves, to give four regions of interest, depicted in red, which were used to

771   analyse NPH3 localisation. Scale bar, 200 μm. **(B)** Quantification of the effect of unilateral blue

772   light irradiation on GFP-NPH3 localisation across the hypocotyl. The number of GFP particles was

773   counted in each of the four regions of interest in etiolated seedlings expressing *NPH3::GFP-NPH3*

774   maintained in darkness (Dark) or irradiated with 0.5 μmol m^{-2} s^{-1} of unilateral blue light for 60 min

775   (Blue). Each value is the mean ± S.E. of 12 seedlings. Asterisks indicate significant differences

776   between the number of GFP particles in the irradiated and shaded hypocotyl sides (* $p < 0.05$; **

777    $p < 0.01$; Student's t-test).

778

779   **Figure 6.** Effect of OKA and de-etiolation on blue-light-induced GFP-NPH3 re-localisation.

780   **(A)** Confocal images of hypocotyl cells of etiolated seedlings expressing *NPH3::GFP-NPH3#1* pre-

781   treated with 1 μM OKA, or solvent-only control (mock) and maintained in darkness (D) or

782   irradiated with 0.5 μmol m^{-2} s^{-1} of blue light for 60 min (L). Scale bar, 50 μm. **(B)** Comparison of

783   blue-light-induced GFP-NPH3 re-localisation in etiolated and de-etiolated seedlings. Confocal

784   images of hypocotyl cells of etiolated and de-etiolated seedlings expressing *NPH3::GFP-NPH3#1*

785   maintained in darkness (D) or irradiated with 0.5 μmol m^{-2} s^{-1} of blue light for 60 min (L). Scale

786   bar, 50 μm. In each case, the quantification of GFP particles is shown on the right. The number of

787   GFP particles was counted in confocal images of hypocotyl cells. Each value is the mean ± S.E. of

788   12 seedlings, and asterisks indicate significant differences between the number of GFP particles

789   between the indicated samples (** $p < 0.01$, Student's t-test).

790

791   **Figure 7.** De-etiolated *rpt2* mutant seedlings show enhanced phototropism and reduced

792   dephosphorylation of NPH3.

793 Phototropism of etiolated and de-etiolated *rpt2* mutant seedlings irradiated with 0.5 µmol m^{-2} s^{-1}

794 ^{1} **(A)** or 0.005 µmol m^{-2} s^{-1} **(B)** of unilateral blue light. Hypocotyl curvatures were measured every

795 20 min for 8 h, and each value is the mean ± S.E. of 20 seedlings. NPH3 phosphorylation status in

796 etiolated (Et) and de-etiolated (De-et) seedlings irradiated with 0.5 µmol m^{-2} s^{-1} **(c)** or 0.005 µmol

797 m^{-2} s^{-1} **(d)** of unilateral blue light. Immunoblot analysis of total protein extracts from etiolated and

798 de-etiolated *rpt2* single-mutant and wild-type (WT) seedlings, maintained in darkness (D) or

799 irradiated with blue light for 60 min (L). Protein extracts were probed with anti-NPH3 antibody.

800

801 **Figure 8.** NPH3 dephosphorylation and hypocotyl curvature responses to increasing fluence rates

802 in etiolated and de-etiolated seedlings.

803 **(A)** Immunoblot analysis of total protein extracts from etiolated and de-etiolated seedlings,

804 maintained in darkness (D) or irradiated with 0.005, 0.5 or 20 µmol m^{-2} s^{-1} of unilateral blue light

805 for 60 min. Protein extracts were probed with anti-NPH3 antibody. Phototropism of etiolated **(B)**

806 and de-etiolated seedlings **(C)** irradiated with 0.005, 0.5 or 20 µmol m^{-2} s^{-1} of unilateral blue light.

807 Hypocotyl curvatures were measured every 10 min for 4 h, and each value is the mean ± S.E. of

808 20 seedlings**.**

809

810 **Figure 9.** Model depicting the correlation between NPH3 phosphorylation status, localisation and

811 phototropic responsiveness.

812 Sustained phosphorylation of NPH3 promotes its action in mediating phototropic signalling from

813 the plasma membrane, whereas NPH3 dephosphorylation reduces it actions by internalising
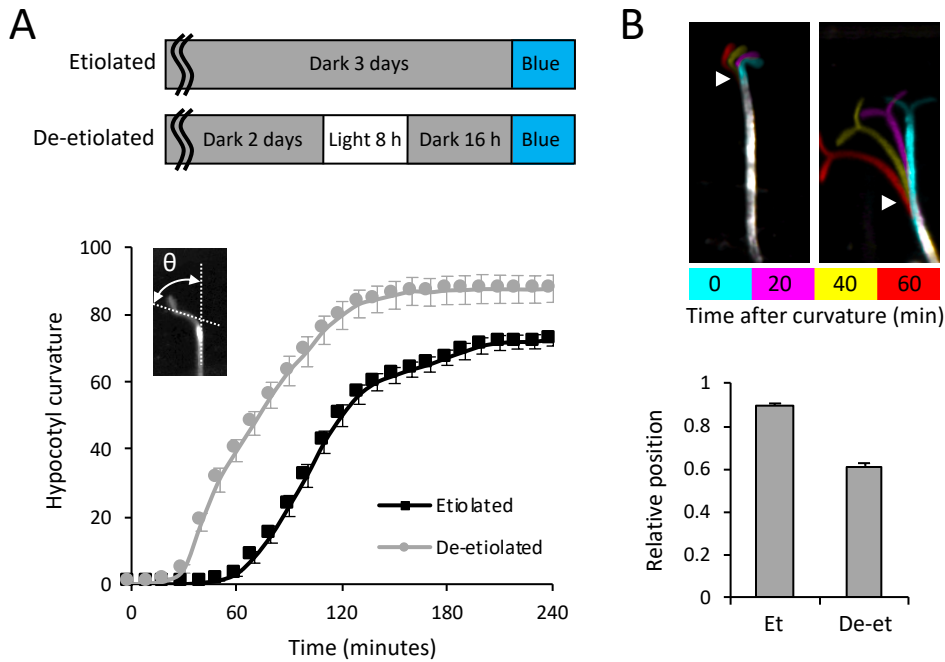
814 NPH3 into aggregates.

Figure 1. De-etiolation enhances phototropism and alters the position of hypocotyl curvature.

(A) Experimental design for analysing phototropism in etiolated and de-etiolated seedlings (top). Etiolated seedlings were grown in darkness for 3 days. For de-etiolated seedlings, de-etiolation was induced in 2-day-old, dark-grown seedlings, with an 8 h white-light treatment (80 µmol m^{-2} s^{-1}), followed by a 16 h dark-adaptation. 3-day-old etiolated and de-etiolated seedlings were placed into unilateral blue light to analyse hypocotyl phototropism. Phototropism of etiolated and de-etiolated seedlings irradiated with 0.5 µmol m^{-2} s^{-1} of unliteral blue light (bottom). Hypocotyl curvatures were measured every 10 min for 4 h, and each value is the mean ± S.E. of 20 seedlings. **(B)** Position of hypocotyl curvature in etiolated (Et) and de-etiolated (De-et) wild-type seedlings (top). Composite image of etiolated (left) and de-etiolated (right) seedling at 0, 20, 40 and 60 min after commencement of curvature. Arrows indicate position of hypocotyl curvature. Quantification of the position of hypocotyl curvature (bottom), as measured from the base of the hypocotyl (with 0 being the closest, and 1 the farthest). The recorded position was divided by total hypocotyl length to give the relative position of curvature. Values are the mean ± S.E. of 20 seedlings.
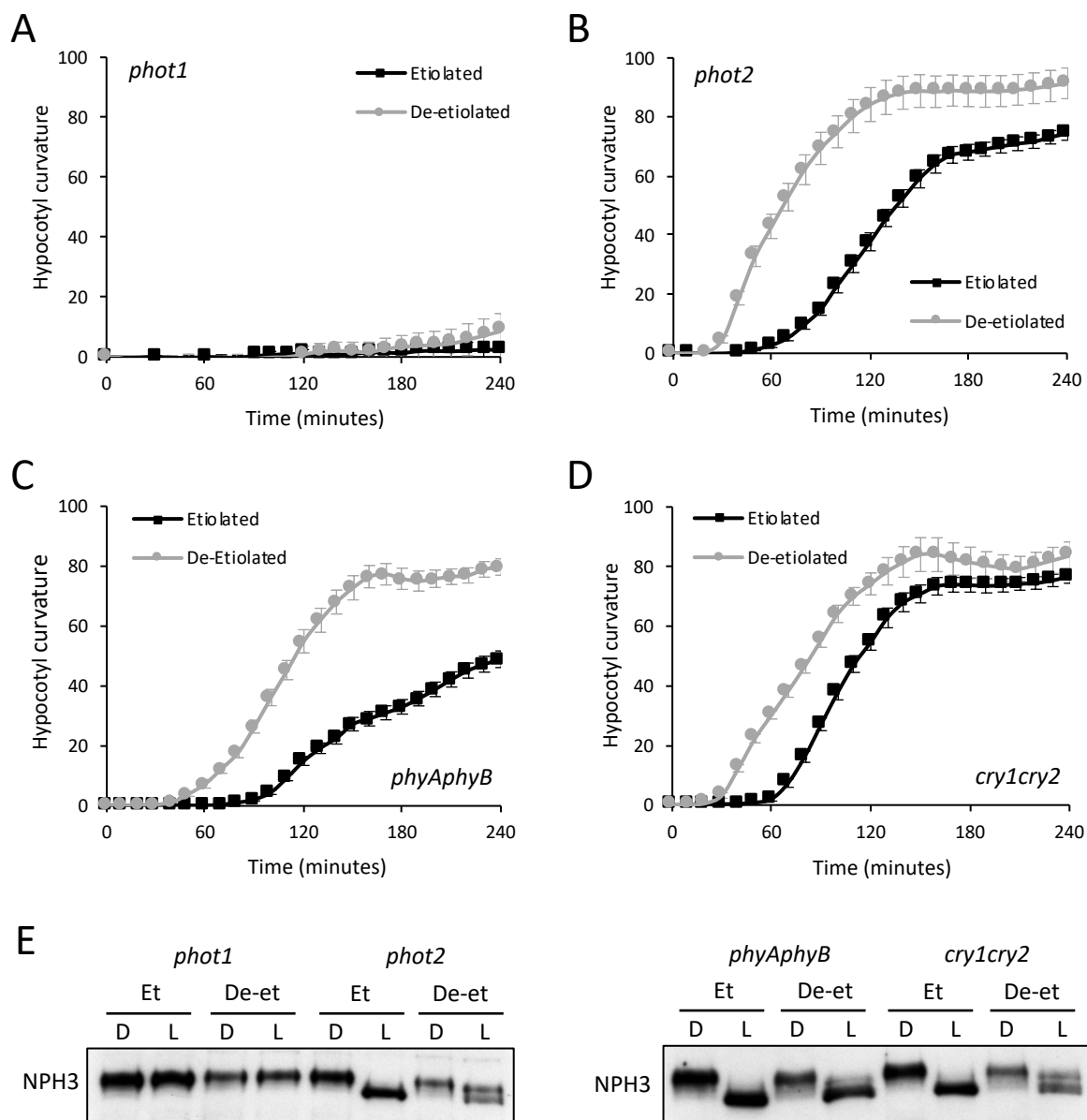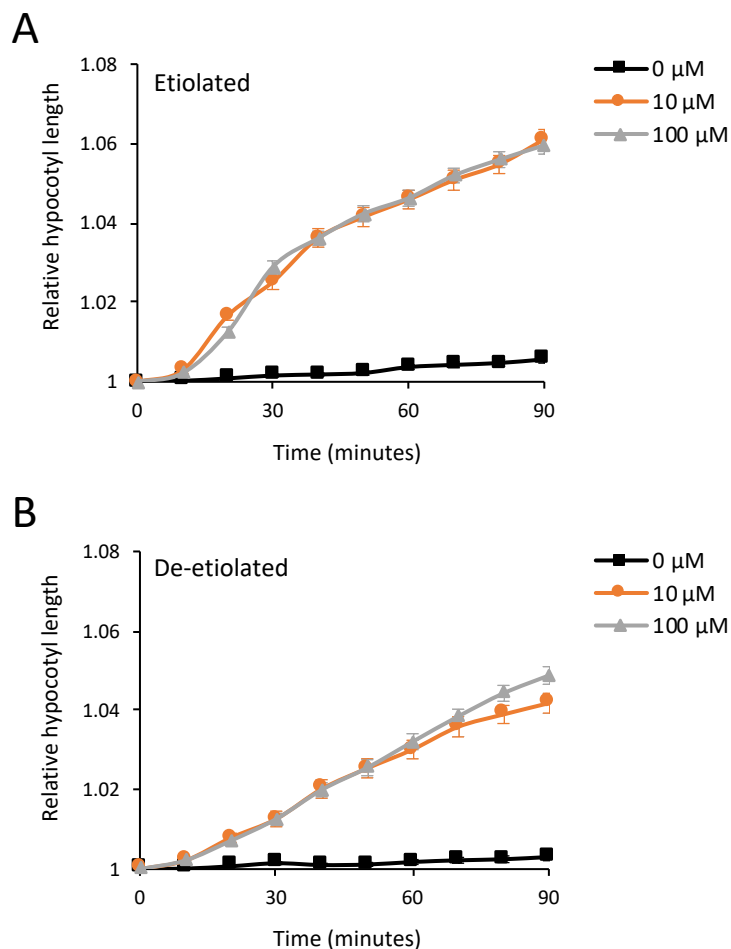
Figure 2. Phototropic responses and NPH3 phosphorylation status in etiolated and de-etiolated seedlings of photoreceptor mutants.

Phototropism of etiolated and de-etiolated *phot1* **(A)** *phot2* **(B)** *phyAphyB* **(C)** and *cry1cry2* **(D)** mutant seedlings, irradiated with 0.5 μmol m^{-2} s^{-1} of unilateral blue light. Hypocotyl curvatures were measured every 10 min for 4 h, and each value is the mean ± S.E. of 17-20 seedlings. **(E)** Immunoblot analysis of total protein extracts from etiolated (Et) and de-etiolated (De-et) *phot1*, *phot2*, *phyAphyB* and *cry1cry2* mutant seedlings, maintained in darkness (D) or irradiated with 0.5 μmol m^{-2} s^{-1} of unilateral blue light for 60 min (L). Protein extracts were probed with anti-NPH3 antibody.
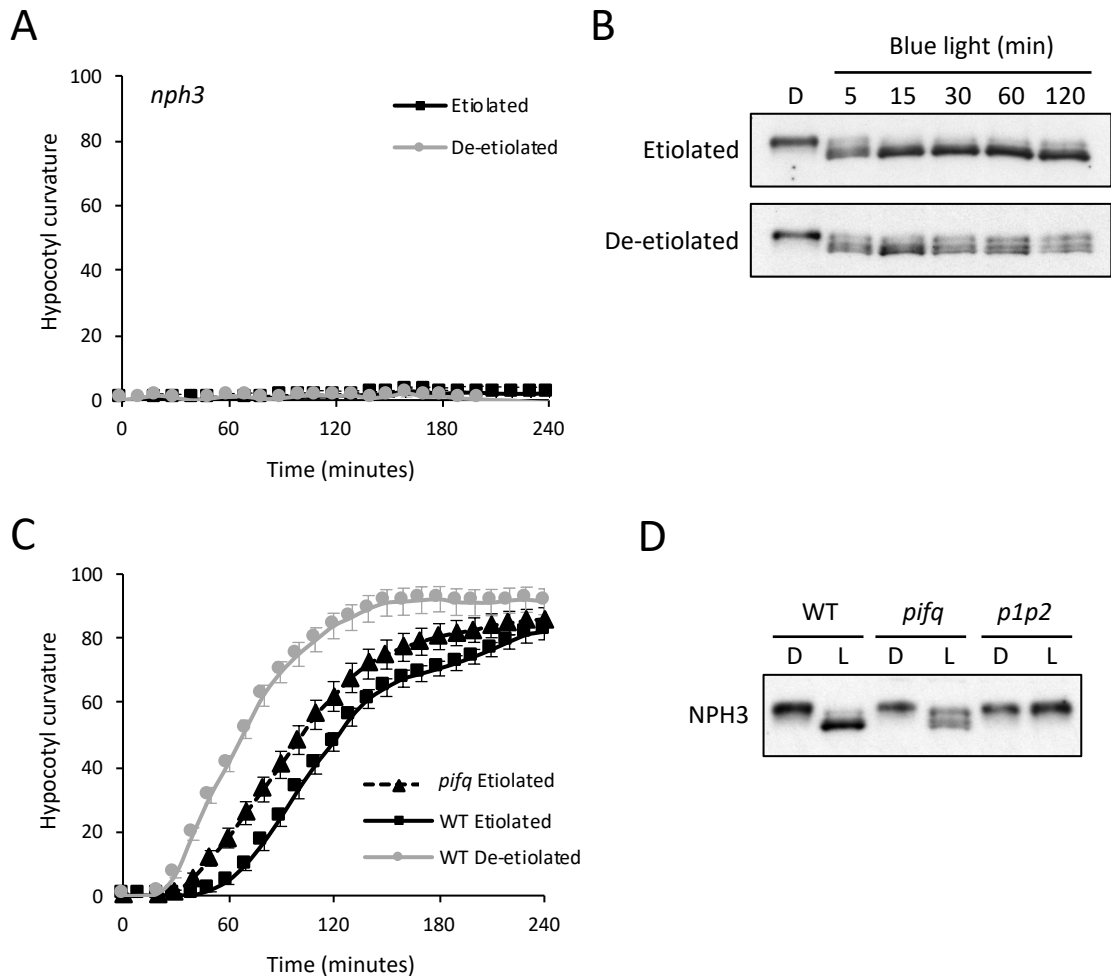
Figure 3. Auxin-induced elongation of hypocotyl segments of etiolated and de-etiolated seedlings.

Elongation of 4 mm apical hypocotyl segments prepared from etiolated **(A)** or de-etiolated **(B)** seedlings. Hypocotyl segments were placed on media containing 0, 10 or 100 μM IAA, and hypocotyl segment lengths were measured every 10 min for 90 min. Each value is the mean ± S.E. of 30 seedlings.

Figure 4. NPH3 functionality and phosphorylation status in etiolated and de-etiolated seedlings.

(A) Phototropism of etiolated and de-etiolated *nph3* mutant seedlings irradiated with 0.5 μmol m^{-2} s^{-1} of unliteral blue light. Hypocotyl curvatures were measured every 10 min for 4 h and each value is the mean ± S.E. of 20 seedlings. **(B)** NPH3 phosphorylation status in etiolated and de-etiolated seedlings during irradiation with blue light . Immunoblot analysis of total protein extracts from etiolated and de-etiolated wild-type seedlings maintained in darkness (D) or irradiated with 0.5 μmol m^{-2} s^{-1} of unilateral blue light for 5, 15, 30, 60 or 120 min. Protein extracts were probed with anti-NPH3 antibody. **(C)** Phototropism of etiolated *pifq* mutant seedlings irradiated with 0.5 μmol m^{-2} s^{-1} of unliteral blue light. Hypocotyl curvatures were measured every 10 min for 4 h and each value is the mean ± S.E. of 20 seedlings. Phototropic responses of etiolated and d-etiolated wild-type (WT) seedlings are also shown. **(D)** Immunoblot analysis of total protein extracts from etiolated wild-type (WT), *pif1 pif3 pif4 pif5* (*pifq*) quadruple mutant, and *phot1phot2 (p1p2)* double mutant seedlings maintained in darkness (D) or irradiated with 0.5 μmol m^{-2} s^{-1} of unilateral blue light for 60 min (L). Protein extracts were probed with anti-NPH3 antibody.
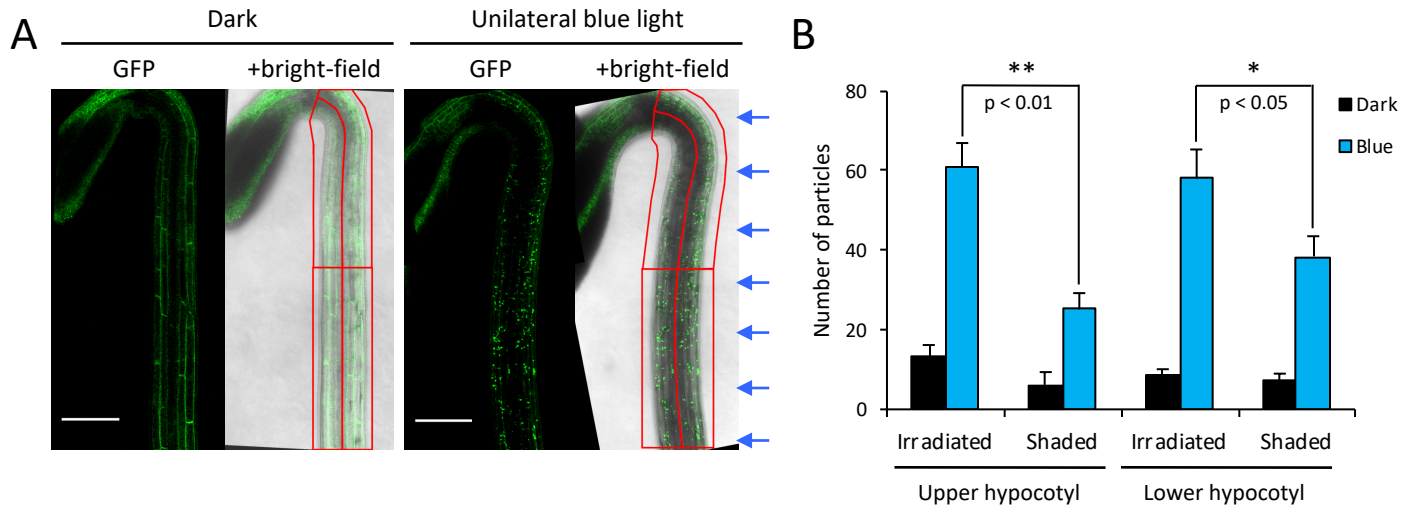
Figure 5. Effect of unilateral blue light irradiation on GFP-NPH3 localisation across the hypocotyl.

(A) Confocal images of etiolated *NPH3::GFP-NPH3#1* seedlings maintained in (left) darkness or (right) irradiated with 0.5 μmol m^{-2} s^{-1} of unilateral blue light for 60 min,. Arrows indicate the direction of blue light. Hypocotyl images were divided into irradiated and shaded sides, and then into upper and lower halves, to give four regions of interest, depicted in red, which were used to analyse NPH3 localisation. Scale bar, 200 μm. **(B)** Quantification of the effect of unilateral blue light irradiation on GFP-NPH3 localisation across the hypocotyl. The number of GFP particles was counted in each of the four regions of interest in etiolated seedlings expressing *NPH3::GFP-NPH3* maintained in darkness (Dark) or irradiated with 0.5 μmol m^{-2} s^{-1} of unilateral blue light for 60 min (Blue). Each value is the mean ± S.E. of 12 seedlings. Asterisks indicate significant differences between the number of GFP particles in the irradiated and shaded hypocotyl sides (* $p < 0.05$; ** $p < 0.01$; Student's t-test).
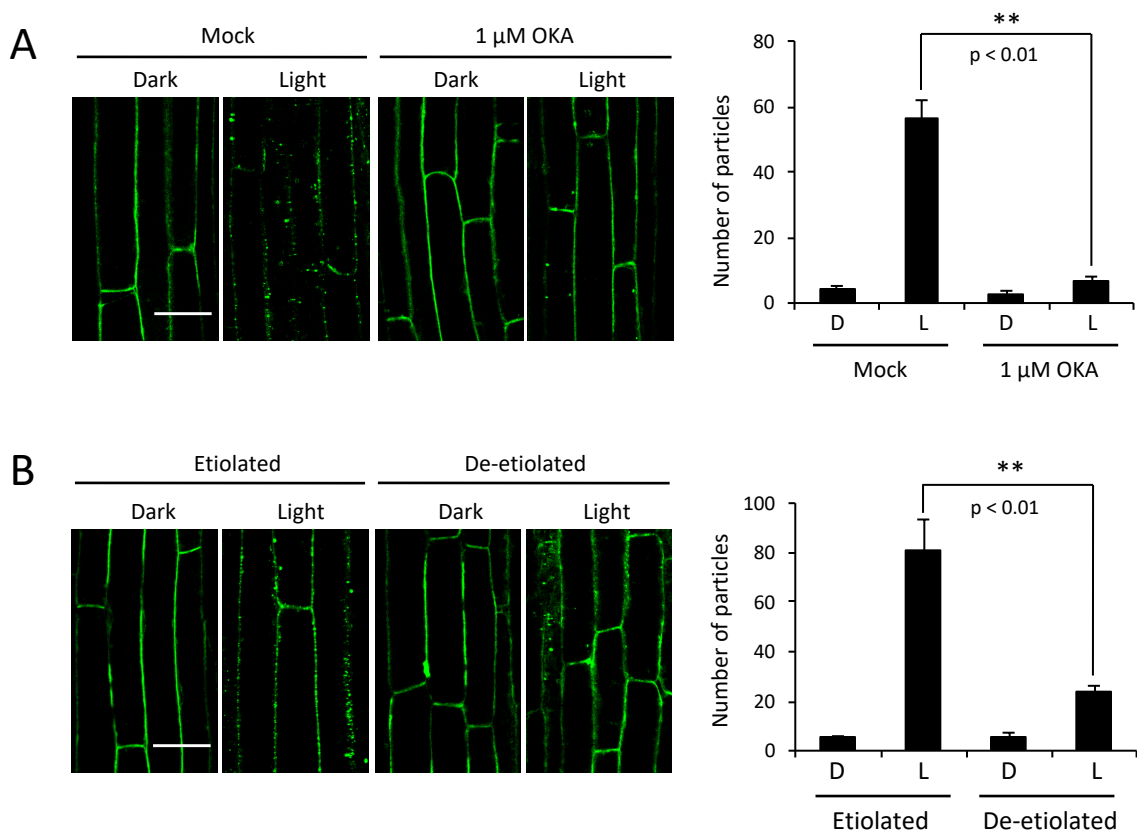
Figure 6. Effect of OKA and de-etiolation on blue-light-induced GFP-NPH3 re-localisation.

(A) Confocal images of hypocotyl cells of etiolated seedlings expressing *NPH3::GFP-NPH3#1* pre-treated with 1 μM OKA, or solvent-only control (mock) and maintained in darkness (D) or irradiated with 0.5 μmol m^{-2} s^{-1} of blue light for 60 min (L). Scale bar, 50 μm. **(B)** Comparison of blue-light-induced GFP-NPH3 re-localisation in etiolated and de-etiolated seedlings. Confocal images of hypocotyl cells of etiolated and de-etiolated seedlings expressing *NPH3::GFP-NPH3#1* maintained in darkness (D) or irradiated with 0.5 μmol m^{-2} s^{-1} of blue light for 60 min (L). Scale bar, 50 μm. In each case, the quantification of GFP particles is shown on the right. The number of GFP particles was counted in confocal images of hypocotyl cells. Each value is the mean ± S.E. of 12 seedlings, and asterisks indicate significant differences between the number of GFP particles between the indicated samples (** $p < 0.01$, Student's t-test).
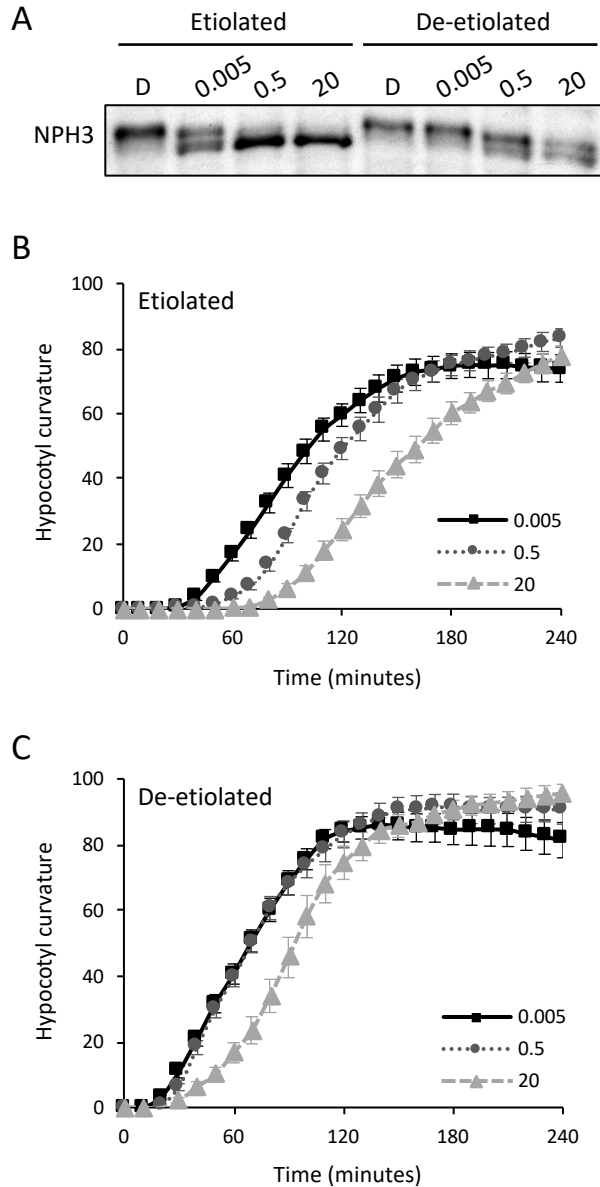
Figure 7. De-etiolated *rpt2* mutant seedlings show enhanced phototropism and reduced dephosphorylation of NPH3.

Phototropism of etiolated and de-etiolated *rpt2* mutant seedlings irradiated with 0.5 μmol m^{-2} s^{-1} **(A)** or 0.005 μmol m^{-2} s^{-1} **(B)** of unilateral blue light. Hypocotyl curvatures were measured every 20 min for 8 h, and each value is the mean ± S.E. of 20 seedlings. NPH3 phosphorylation status in etiolated (Et) and de-etiolated (De-et) seedlings irradiated with 0.5 μmol m^{-2} s^{-1} **(c)** or 0.005 μmol m^{-2} s^{-1} **(d)** of unilateral blue light. Immunoblot analysis of total protein extracts from etiolated and de-etiolated *rpt2* single-mutant and wild-type (WT) seedlings, maintained in darkness (D) or irradiated with blue light for 60 min (L). Protein extracts were probed with anti-NPH3 antibody.
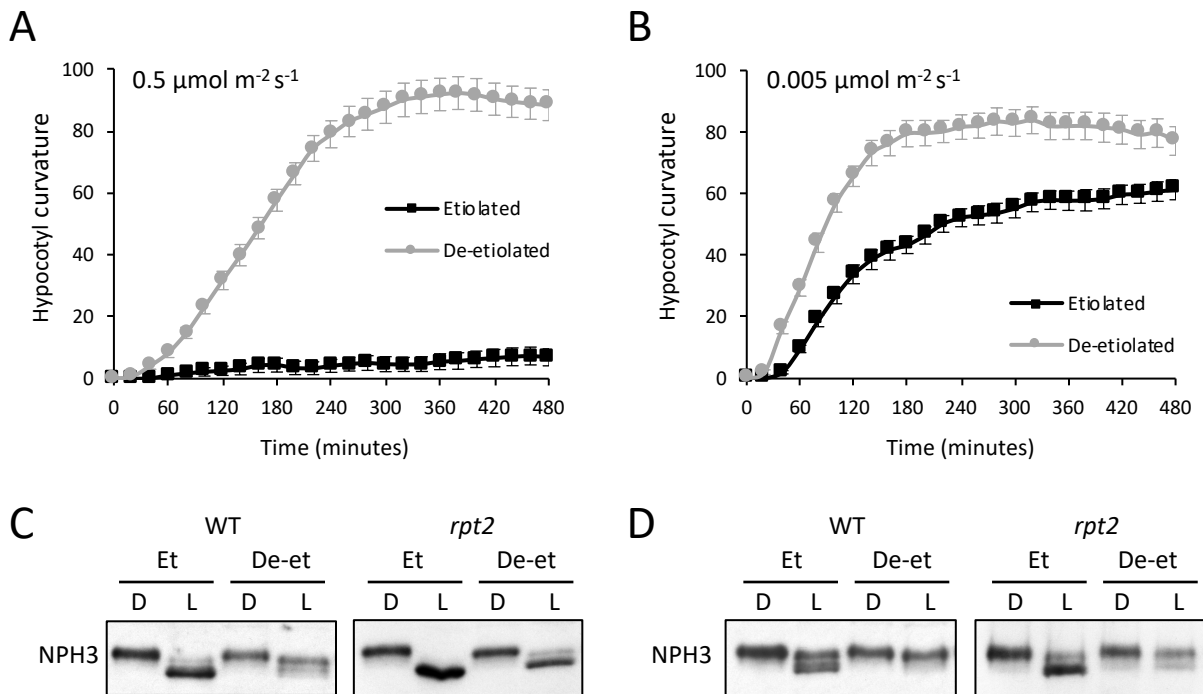
Figure 8. NPH3 dephosphorylation and hypocotyl curvature responses to increasing fluence rates in etiolated and de-etiolated seedlings.

(A) Immunoblot analysis of total protein extracts from etiolated and de-etiolated seedlings, maintained in darkness (D) or irradiated with 0.005, 0.5 or 20 μmol m^{-2} s^{-1} of unilateral blue light for 60 min. Protein extracts were probed with anti-NPH3 antibody. Phototropism of etiolated **(B)** and de-etiolated seedlings **(C)** irradiated with 0.005, 0.5 or 20 μmol m^{-2} s^{-1} of unilateral blue light. Hypocotyl curvatures were measured every 10 min for 4 h, and each value is the mean ± S.E. of 20 seedlings**.**
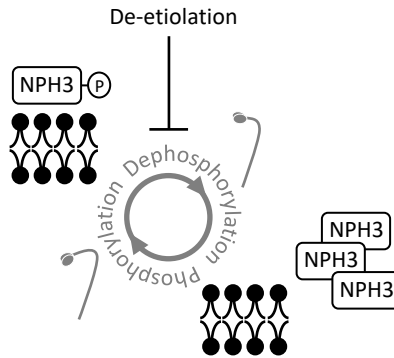
Figure 9. Model depicting the correlation between NPH3 phosphorylation status, localisation and phototropic responsiveness.

Sustained phosphorylation of NPH3 promotes its action in mediating phototropic signalling from the plasma membrane, whereas NPH3 dephosphorylation reduces it actions by internalising NPH3 into aggregates.